Electronic Supplementary Information for Journal of Materials Chemistry A

Heteroepitaxially Grown Two-Dimensional Metal-Organic Framework and Its Derivative for Electrocatalytic Oxygen Reduction Reaction

*Meiling Huo,[†, [a]] Tu Sun,[†, [b]] Yanzhi Wang,[†, [a]] Pengfei Sun,[a] Jinshuang Dang,[a] Bin Wang,[a] N. V. R. Aditya Dharanipragada,[c] A. Ken Inge,[c] Wei Zhang,[a] Rui Cao,[a] Yanhang Ma,[b][d], * and Haoquan Zheng[a][e], **

[a]Key Laboratory of Applied Surface and Colloid Chemistry, Ministry of Education, School of Chemistry and Chemical Engineering, Shaanxi Normal University, Xi'an 710119, China

[b]School of Physical Science and Technology, ShanghaiTech University, Shanghai 201210, China

[c]Department of Materials and Environmental Chemistry, Stockholm University, SE−10691 Stockholm, Sweden

[d]Shanghai Key Laboratory of High-resolution Electron Microscopy, ShanghaiTech University; Shanghai, 201210, People Republic of China.

[e]International Joint Research Center on Advanced Characterizations of Xi'an City, School of Chemistry and Chemical Engineering, Shaanxi Normal University, Xi'an 710119, China

†These authors have contributed equally to this work.

*Corresponding Author(s): mayh2@shanghaitech.edu.cn; zhenghaoquan@snnu.edu.cn

Preparation of Electrodes

The preparation method of working electrode: 10 mg of catalyst was added to 1 mL of mixed solution (containing 900 μL isopropanol, 80 μL deionized water, and 20 μL Nafion aqueous solution (5 wt%)). The mixed solution was sonicated for 30 minutes to form a homogeneous suspension. 20 μL of the catalyst solution was droped on the rotating disk electrode (RDE) electrode (catalyst loading is about 0.4 mg cm⁻²). After natural drying, a homogeneous film was formed.

The scanning rate of linear sweep voltammetry (LSV) curves was 5 mV s⁻¹, and the scanning rate of cyclic voltammetry (CV) curves was 50 mV s⁻¹. iR compensation at 100% for LSV measurement. The electrolyte concentration was 0.1 M KOH. Electrochemical Impedance Spectroscopy (EIS) measurement frequency was in the range of 0.1 Hz and 10,000 Hz.

The electron transfer numbers (n) was calculated with Koutecky-Levich (K-L) equation:

$$\frac{1}{j} = \frac{1}{j_l} + \frac{1}{j_k} = \frac{1}{B\omega^{1/2}} + \frac{1}{j_k}$$

where j is the measured current density; j_l is the diffusion current density; j_k is the kinetic current density; ω is the rotation speed in rpm; B can be confirmed by K-L equation:

$$B = 0.2nFC_0(D_0)^{2/3}v^{-1/6}$$

where n is the transfer numbers; F is the Faraday constant (96485 C mol⁻¹); C_o is the concentration of O_2 in 0.1 M KOH (1.2×10^{-6} mol cm⁻³); D_o is the diffusion coefficient of O_2 in 0.1 M KOH (1.9×10^{-5} cm² s⁻¹); υ is the viscosity of 0.1 M KOH (0.1 cm² s⁻¹). Afterwards, n can be obtained by the equation.
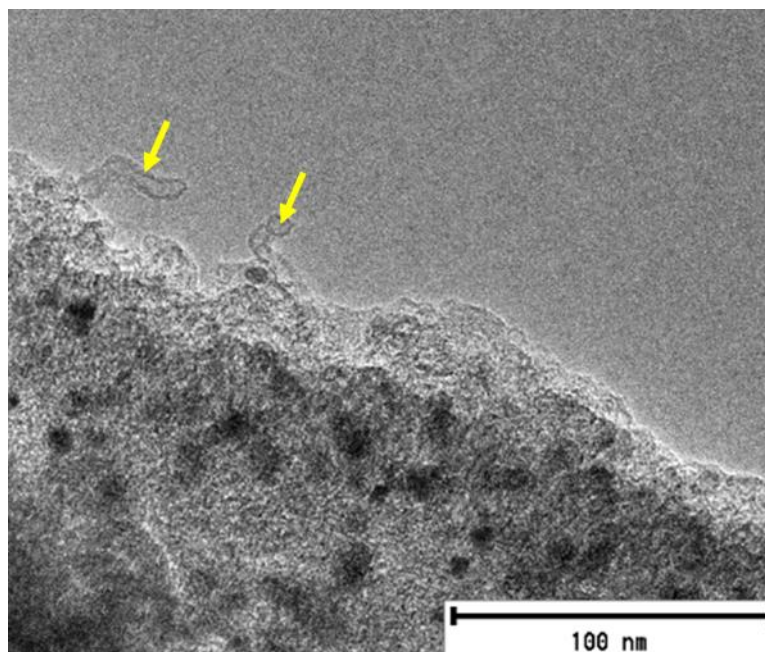
The n can be obtained by another equation:

$$H_2O_2(\%) = 200 \times \frac{\frac{I_r}{N}}{I_d + \frac{I_r}{N}}$$
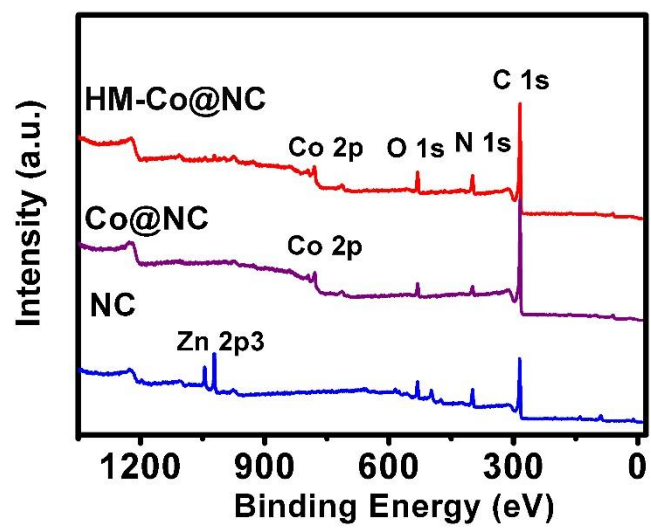
$$n = 4 \times \frac{I_d}{I_d + \frac{I_r}{N}}$$

i_d is the disk current; i_r is the ring current; N is the capture coefficient and it is about 0.37.
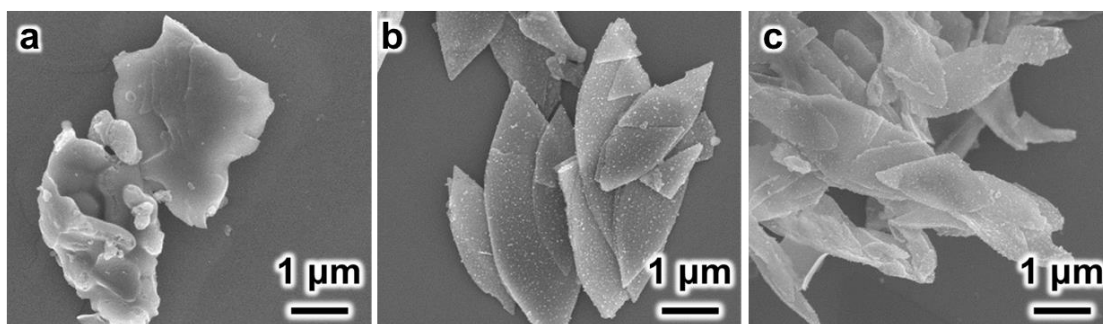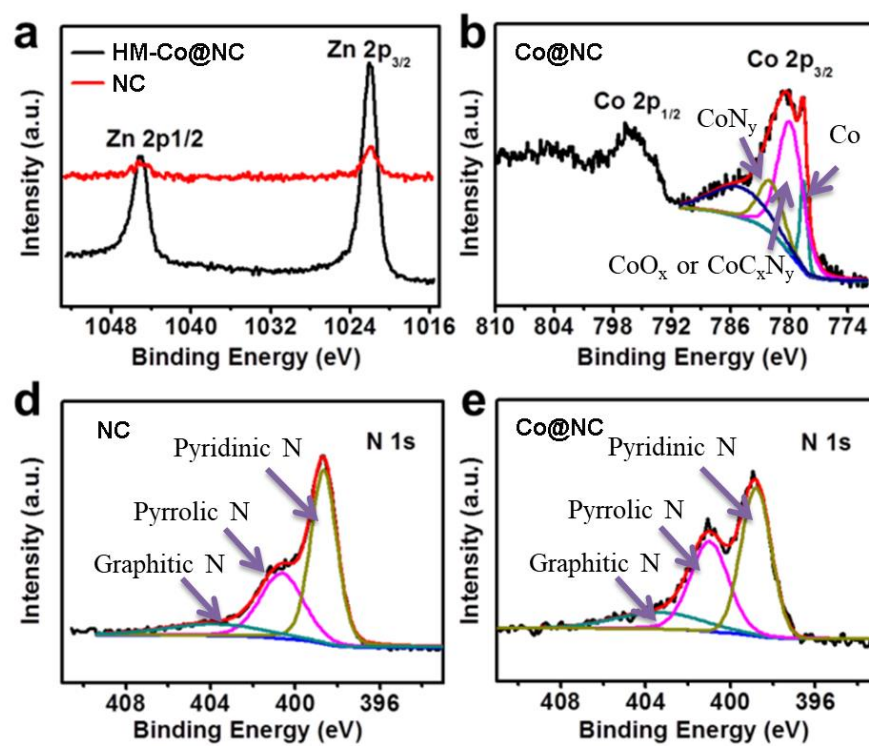
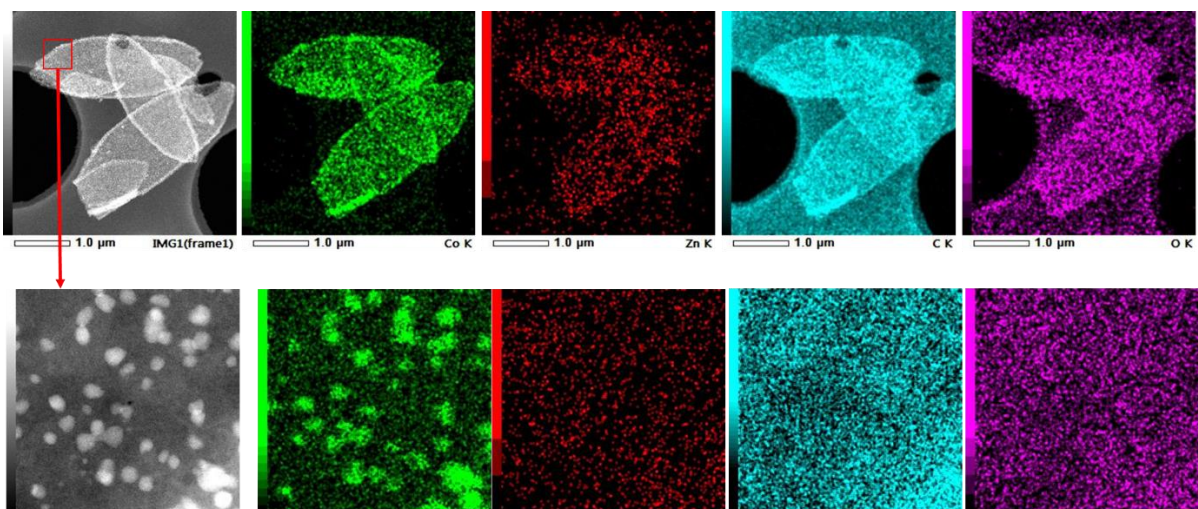**Fig. S1.** SEM images of NC (a), Co@NC (b), and HM-Co@NC (c).
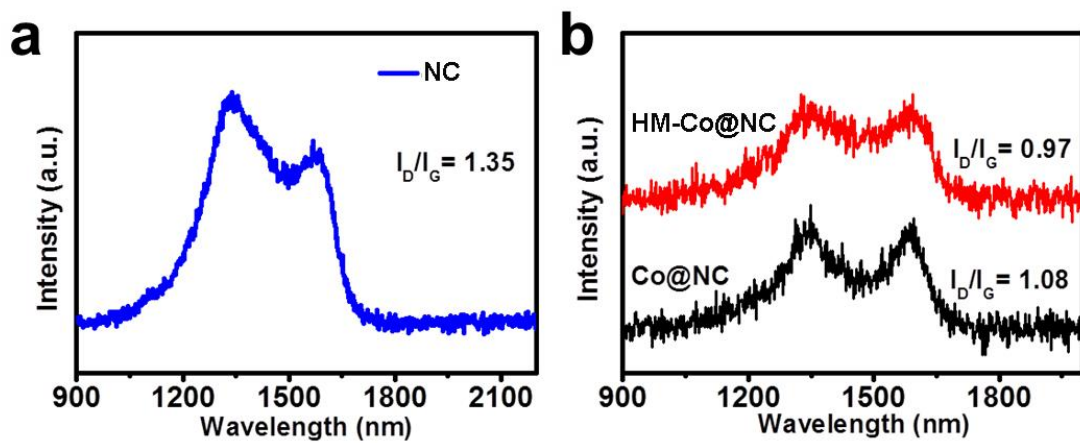
Fig. S2. HRTEM image of HM-Co@NC.

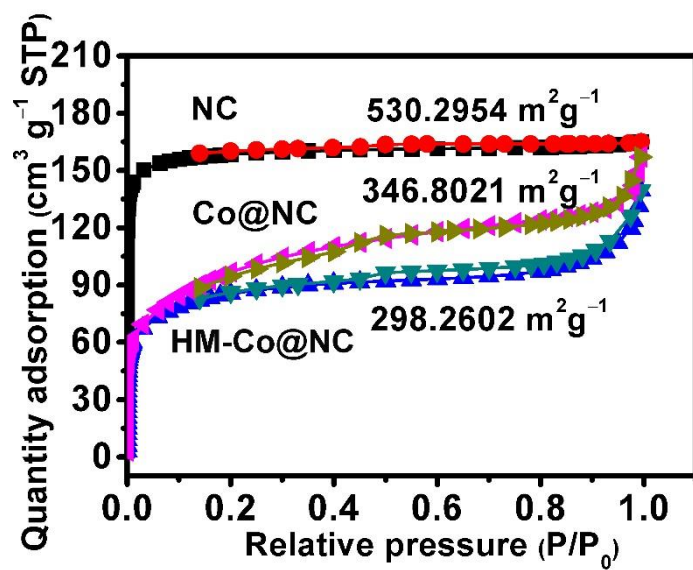**Fig. S3.** XPS spectra of NC, Co@NC, and HM-Co@NC.

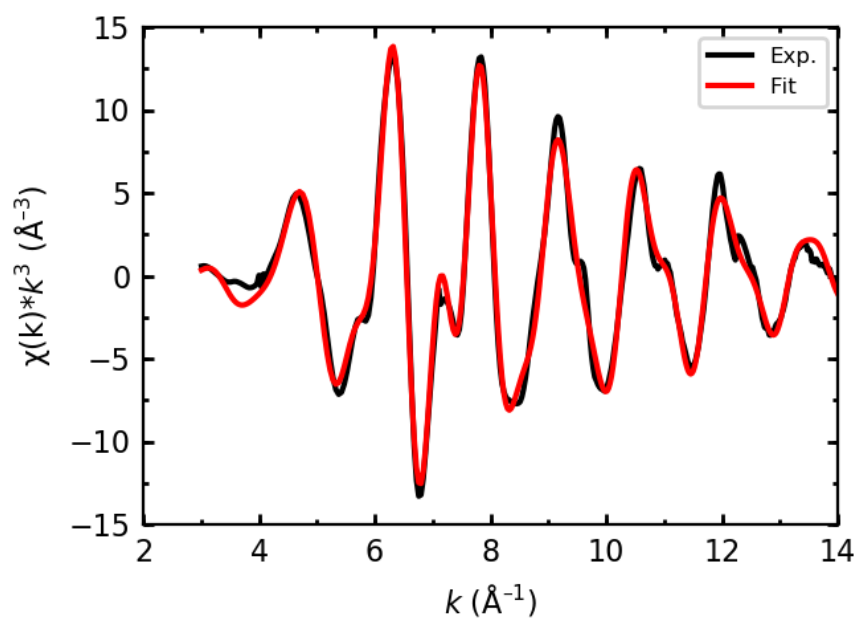**Fig. S4.** High-resolution XPS spectra of NC, Co@NC, and HM-Co@NC.

Fig. S5. STEM image and EDS mapping of HM-Co@NC.

**Fig. S6.** Raman spectra of NC (a), Co@NC, and HM-Co@NC (b).

Fig. S7. N$_2$ adsorption/desorption isotherms of NC, Co@NC, and HM-Co@NC.

Fig. S8. Co K-edge k^3-weighted EXAFS spectrum of HM-Co@NC. Black curve – experimental, red curve – model.

The peaks at longer distances are derived from single scatterings of Co---Co in metal shells further out than the first shell and multiple scatterings among Co atoms.
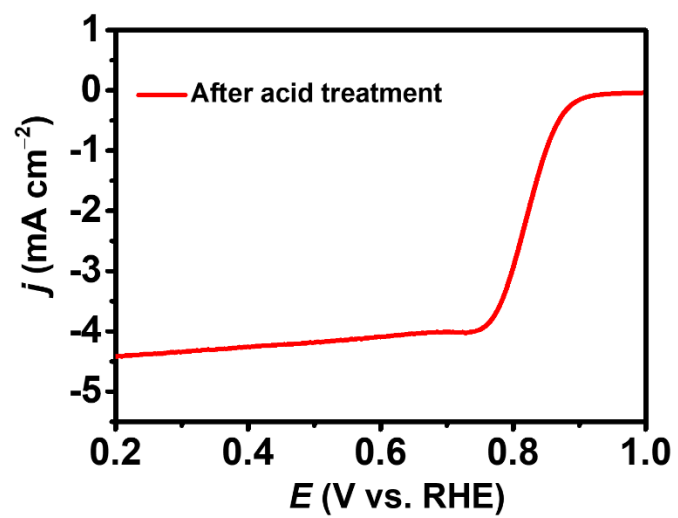
Fig. S9. LSV curves of HM-Co@NC after being treated in 1 M H_2SO_4 at 70 ^{o}C for 20 h. The $E_{1/2}$ = 0.82 V.
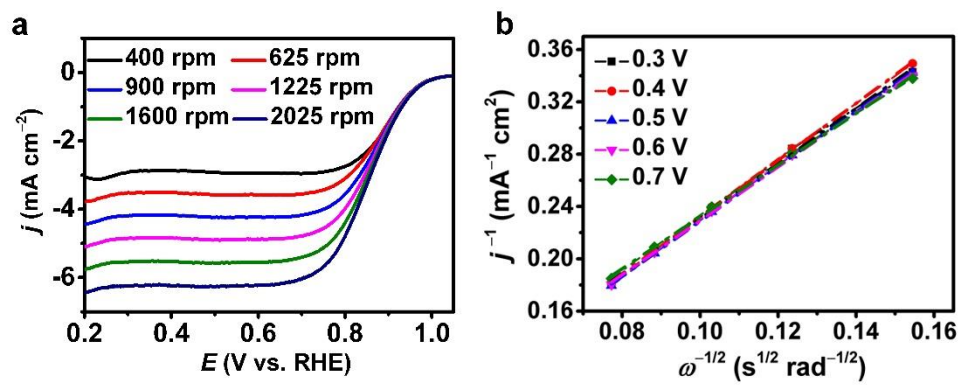
Fig. S10. (a) LSV curves of Pt/C at various rotation speeds. (b) K-L plots of Pt/C at various potentials.
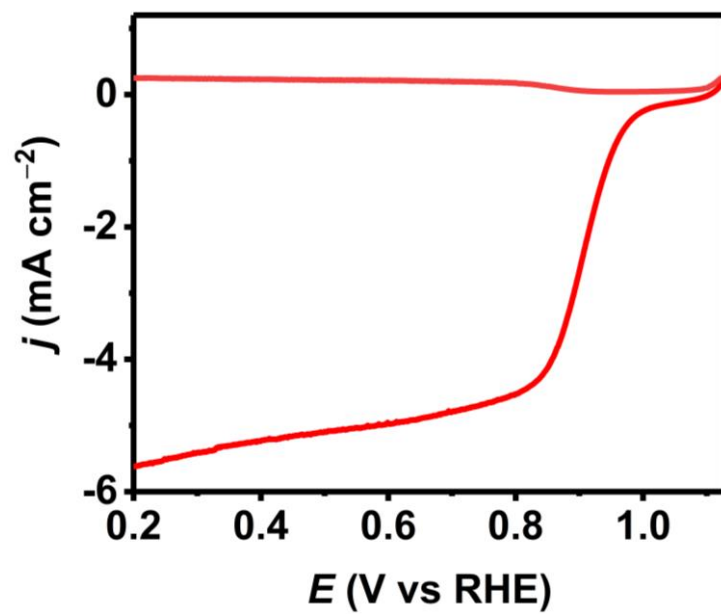
Fig. S11. RRDE polarization curve of HM-Co@NC at 1600 rpm in O_2-saturated 0.1 M KOH.
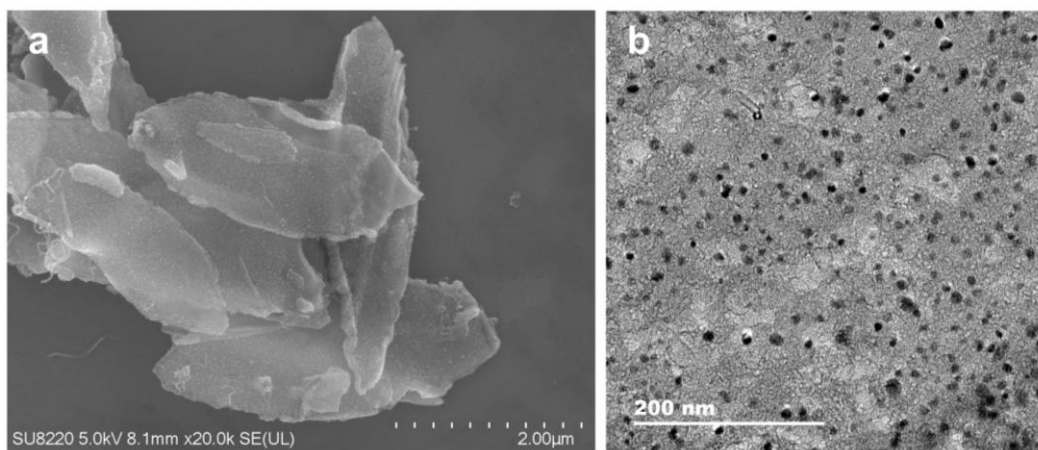
Fig. S12. SEM (a) and TEM images (b) of HM-Co@NC after catalysis.

Fig. S13. LSV curves of HM-Co@NC (red line) and Co, N doped carbon derived from ZIF-L-Zn@ZIF-67 (black line).

Table S1. Mean number of distances, **N**, mean distances, **d** (Å), and Debye-Waller coefficients, **σ^2** (Å^2), Many-body amplitude reduction factor, S_0^2, in the EXAFS 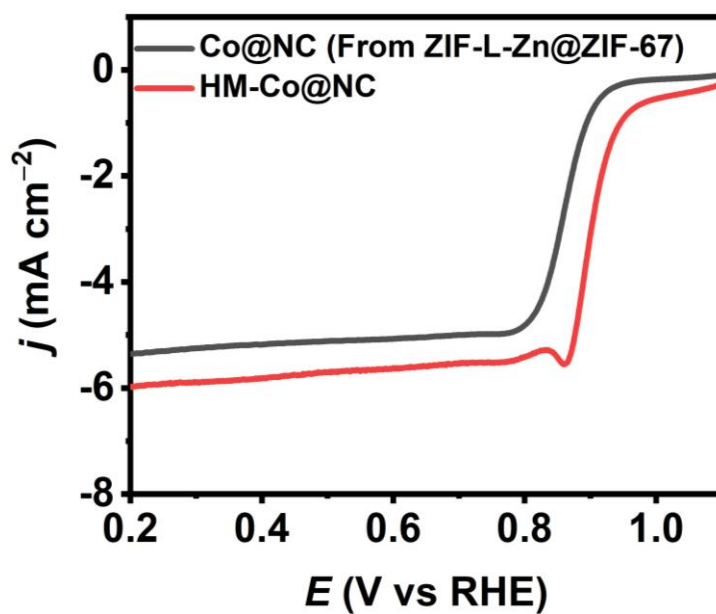refinement of the first coordination shell. S_0^2 was refined at 0.76(2). This value was consistent with S_0^2 value derived from the EXAFS refinement of Co foil with known structures. The standard deviations in parentheses were obtained from k^3-weighted least square refinement of the EXAFS function χ(k) and do not include systematic errors of the measurement. Underscored parameters were optimized from several trials and were fixed in the individual refinements. The signals include single scatterings of the first three shells. Other scattering signals are not shown in the table due to minor contributions or long distances.

Sample	Signal	N	d (Å)	σ² (Å²)
HM-Co@NC	Co–O/N/C	0.5	1.962(7)	0.0017(7)
	Co–Co (first shell)	6.0	2.486(1)	0.0064(1)
	Co---Co (second shell)	3.0	3.507(7)	0.0135(9)
	Co---Co (third shell)	10	4.365(3)	0.0101(3)

However, it is beyond the limit of the EXAFS data to resolve Co–N and Co–C as they have very similar bond lengths. The EXAFS refinement parameters of the first coordination shell are presented in Table S1. The presence of small amount of Co–O is possible due to partial oxidized Co by residual O_2 or the adsorbed O_2 from air.

Table S2. Comparison of the ORR performance of HM-Co@NC catalysts from literature and this work.

Catalyst	Electrolyte	$E_{1/2}$ vs RHE	Ref
HM-Co@NC	0.1 M KOH	**887 mV**	**This work**
Co_4N/C	1 M KOH	875 mV	*J. Am. Chem. Soc. 2019, 141, 19241-19245*
Fe-N-C	0.1 M KOH	850 mV	*J. Am. Chem. Soc. 2019, 141, 2035-2045*
$Co_{1.5}Mn_{1.5}O_4/C$	1 M KOH	850 mV	*J. Am. Chem. Soc. 2019, 141, 1463-1466*
Fe@Aza-PON	0.1 M KOH	839 mV	*J. Am. Chem. Soc. 2018, 140, 1737-1742*
C_{60}-$SWCNT_{15}$	0.1 M KOH	840 mV	*J. Am. Chem. Soc. 2019, 141, 11658-11666*
D-AC@2Mn-4Co	0.1 M KOH	803 mV	*Adv. Mater. **2016**, 28, 8771–8778*
W_2N/WC	0.1 M KOH	810 mV	*Adv. Mater. **2019**, 1905679*
NiCo-NLG-270	0.1 M KOH	820 mV	*Adv. Mater. **2018**, 30, 1800005*
$Co_3InC_{0.7}N_{0.3}$	0.1 M KOH	854 mV	*Angew. Chem. Int. Ed. 2019, 58, 2 – 9*
Zn-N-C-1	0.1 M KOH	873 mV	*Angew. Chem. Int. Ed. 2019, 58, 7035 –7039*

Table S3. The performance of electrically rechargeable Zn-air batteries with various bifunctional electrocatalysts. The corresponding current densities (mA cm^{-2}) for voltage gap and specific capacity are also listed in the Table (after @ in each table cell).

Catalyst	Charge/discharge voltage gap (V)	Peak power density (mW cm^{-2})	Specific capacity (mAh g^{-1})	Ref
HM-Co@NC	0.84@2	**209.4**	**770.2@20**	**This work**
NiFe$_2$O$_4$/FeNi$_2$S$_4$ HNSs	1@2	187	--	*J. Am. Chem. Soc.* 2018, 140, 17624-17631
W$_2$N/WC	1.25@10	172	749@10	*Adv. Mater.* **2019**, 1905679
NiCo-NLG-270	0.8@2	103	403@10	*Adv. Mater.* **2018**, 30, 1800005
Co/CNF	0.9@5	163	680@20	*Adv. Mater.* **2019**, 31, 1808043
NC@Co-NGC DSNCs	0.85@2	109	537@20	*Adv. Mater.* **2017**, 29, 1700874
Co$_4$N/CNW/CC	1.09@50	174	774@10	*J. Am. Chem. Soc.* 2016, 138, 10226-10231
Ni-Fe-MoN NTs	0.93@10	118	753.7@10	*Adv. Energy Mater.* **2018**, 8, 1802327
NGM-Co	1.12@5	152	749.4@20	*Adv. Mater.* **2017**, 29, 1703185
Fe-N$_4$ SAs/NPC	1.45@50	232	--	*Angew. Chem. Int. Ed. 2018, 57, 8614 – 8618*
meso/micro-FeCo-N$_x$-CN-30	0.91@20	150	--	*Angew. Chem. Int. Ed. 2018, 57, 1856 – 1862*